

First trigonal-antiprismatic tris-dichloroglyoximate iron(II) clathrochelate and its reactivity in nucleophilic substitution reactions†

Yan Z. Voloshin,^{a*} Oleg A. Varzatskii,^b Aleksei V. Palchik,^b Nataly G. Strizhakova,^b Ivan I. Vorontsov,^c Mikhail Yu. Antipin,^c Dmitry I. Kochubey^d and Boris N. Novgorodov^d

^a Karpov Institute of Physical Chemistry, 10 Vorontsovo Pole, 105064, Moscow, Russia.

E-mail: voloshin@cc.nifhi.ac.ru

^b Vernadskii Institute of General and Inorganic Chemistry, 03680, Kiev-142, Ukraine

^c Nesmeyanov Institute of Organoelement Compounds, 119991, Moscow, Russia

^d Borekov Institute of Catalysis, Siberian Branch of the Russian Academy of Sciences, 630090, Novosibirsk, Russia

Received (in Montpellier, France) 22nd November 2002, Accepted 5th February 2003

First published as an Advance Article on the web 3rd June 2003

Tris-dichloroglyoximate clathrochelate $[\text{Fe}(\text{Cl}_2\text{Gm})_3(\text{SnCl}_3)_2]^{2-}$ dianion has been synthesized by a procedure differing from those described earlier for boron-capped analogs. The co-ordinately saturated SnCl_6^{2-} dianion is now used as the capping agent instead of boron-containing Lewis acids. The tris-dichloroglyoximate tin-capped product obtained is far less reactive than its boron-capped analogs, and only in the case of a thiophenolate anion was the “regular” hexafunctionalized clathrochelate obtained. The complexes synthesized have been characterized by elemental analysis, PD and MALDI-TOF mass, IR, UV-vis and ^1H , ^{13}C and ^{119}Sn NMR spectra, cyclic voltammetry, and X-ray crystallography for the clathrochelate $[\text{Fe}(\text{Cl}_2\text{Gm})_3(\text{SnCl}_3)_2]^{2-}$ dianion. The geometry of the functionalized complex (the distortion angle ϕ and main bond lengths in the clathrochelate framework) has been deduced from the quadrupole splitting value in the ^{57}Fe Mössbauer spectrum and EXAFS data, respectively.

Introduction

A suitable reactive halogenide precursor has proved to be an essential reagent in the directed synthesis of ribbed-functionalized (*i.e.*, functionalization of chelate α -dioximate fragments) clathrochelate d-metal tris-dioximates with varied structural, chemical, and physicochemical characteristics. The use of such a strategy has allowed us to obtain both triribbed- (*i.e.*, functionalization of all three dioximate fragments) and mono-ribbed- (*i.e.*, functionalization of only one of these fragments) functionalized macrobicyclic complexes of Fe^{2+} , Ru^{2+} , Co^{2+} and Co^{3+} ions starting from hexa- and dichloro clathrochelate precursors, respectively (Scheme 1).^{1–5} Moreover, since all of the previously obtained complexes containing boron-capping groups possessed a geometry approaching that of the trigonal prism (TP),⁶ it seemed that the geometry of the resultant functionalized complexes was predominantly determined by that of their precursors. Therefore, we thought that it was desirable to synthesize a tin-capped reactive precursor to obtain trigonal-antiprismatic ribbed-functionalized clathrochelates since the geometry of all previously obtained tin-capped clathrochelates approaches that of the trigonal antiprism (TAP).^{7–10}

Experimental

General procedures

The reagents used, $\text{FeCl}_2 \cdot 4\text{H}_2\text{O}$, SnCl_4 , $\text{C}_6\text{H}_5\text{SH}$, $[(\text{CH}_3)_4\text{N}]\text{Cl}$, $[(\text{CH}_3)_2\text{N}]_4\text{P}]\text{BF}_4$ and $[(n\text{-C}_4\text{H}_9)_4\text{N}]\text{Cl}$, as well as the

organic solvents, were obtained commercially (Fluka). Dichloroglyoxime (denoted as $\text{H}_2\text{Cl}_2\text{Gm}$) was prepared by chlorination of glyoxime as described in ref. 11. The $\text{Fe}(\text{CH}_3\text{CN})_4\text{Cl}_2$ salt was obtained as described in ref. 2.

Analytical data (C, H, N content) were obtained with a Carlo Erba model 1106 microanalyzer. Iron content was determined spectrophotometrically.

The plasma desorption (PD) mass spectra were recorded using a BC MS SELMI time-of-flight mass spectrometer and an accelerating voltage of 20 kV. Ionization was induced by ^{252}Cf spontaneous decay fragments, and typically 20 000 decay acts were registered. The samples (approximately 1–2 mg) were applied to a gilded disk or to a nitrocellulose layer.

The IR spectra of solid samples (KBr tablets) in the range of 400–4000 cm^{-1} were recorded with a Specord M-80 Carl Zeiss spectrophotometer. The UV-vis spectra of solutions in methylene dichloride and acetonitrile were recorded in the 230–800 nm range with a Lambda 9 Perkin Elmer spectrophotometer. The individual Gaussian components of these spectra were calculated using the SPECTRA program.

The ^1H , ^{13}C and ^{11}B NMR spectra were recorded from CD_3CN and CD_2Cl_2 solutions with a Bruker AC-200 FT-spectrometer.

^{57}Fe Mössbauer spectra were obtained with a YGRS-4M spectrometer in constant acceleration mode. The spectra were collected with a 256-multichannel amplitude analyzer. The isomer shift was measured relative to sodium nitroprusside and an $\alpha\text{-Fe}$ foil was used for the velocity scale calibration. ^{57}Co in a chromium matrix was used as the source and was always kept at 298 K. The minimal absorption line width in the spectrum of a standard sample of sodium nitroprusside was 0.24 mm s^{-1} .

† Electronic supplementary information (ESI) available: EXAFS oscillations, $k^2\chi(k)$, and RDA curves of six boron- and tin-capped iron(II) clathrochelates. See <http://www.rsc.org/suppdata/nj/b2/b211623e/>



The EXAFS spectra of the iron and tin K-edges for all samples studied were obtained at the EXAFS Station of the Siberian Synchrotron Radiation Center. The storage ring VEPP-3 with an electron beam energy of 2 GeV and an average stored current of 80 mA was used as the source of radiation. The X-ray energy was monitored with a channel-cut Si(111) monochromator. The EXAFS spectra were recorded in transmission mode with 1.4 eV steps and treated using the standard procedures in the VIPER program.¹³ The background was removed by extrapolating the pre-edge region into the EXAFS region using Victoreen's polynomials. Three cubic splines were used to construct the smooth part of the adsorption coefficient. The inflection point of the edge of the X-ray absorption spectrum was used as the initial point ($k = 0$) of the EXAFS spectrum. The radial distribution function of atoms (RDA) was calculated from the EXAFS spectra in $k^2\chi(k)$ as the modulus of the Fourier transform in the wave number interval 3.0–13.0 Å⁻¹. A curve-fitting procedure with EXCURV-92 code¹⁴ was employed to determine the distances and coordination numbers.

$[(n\text{-C}_4\text{H}_9)_4\text{N}]_2[\text{Fe}(\text{Cl}_2\text{Gm})_3(\text{SnCl}_3)_2]$ (I). $\text{Fe}(\text{CH}_3\text{CN})_4\text{Cl}_2$ (2.90 g, 10 mmol) and an excess of $\text{H}_2\text{Cl}_2\text{Gm}$ (5.20 g, 33 mmol) were dissolved/suspended with intensive stirring in dry nitromethane (100 ml) under argon. The reaction mixture was then boiled and an excess of $[(\text{CH}_3)_4\text{N}]_2\text{SnCl}_6$ (10.1 g, 21 mmol) was added. The brown-red reaction mixture was heated and stirred for 6 h and then cooled to 25 °C. Diethyl ether (100 ml) was then added and the reaction mixture was filtered. The precipitate was extracted with dimethylsulfoxide and the solution

[(CH₃)₂N]₄P]₂[Fe(Cl₂Gm)₃(SnCl₃)₂] (2). This complex was synthesized by a similar procedure except that [(CH₃)₂N]₄P[BF₄] salt was used instead of [(*n*-C₄H₉)₄N]Cl (yield: 7.2g, 52%). Anal. calcd. for C₂₂H₄₈N₁₄O₆Cl₁₂FeP₂Sn₂: C, 19.06; H, 3.47; N, 14.15; Fe, 4.03; found: C, 19.14; H, 3.46; N, 14.02; Fe, 4.11%. MS(PD): *m/z* (positive) 1592 [M + {(CH₃)₂N]₄P]⁺, *m/z* (negative) -972 [M - 2{(CH₃)₂N]₄P + H]⁻, -936 [M - 2((CH₃)₂N)₄P - Cl]⁻. ¹H NMR (CD₂Cl₂): δ 2.60 (d, *J*_{H-³¹P} = 9.7 Hz). ¹³C{¹H} NMR (CD₂Cl₂): δ 37.6 (d, *J*_{13C-³¹P} = 4.3 Hz, CH₃), 131.0 (s, ClC=N). UV-vis (CH₂Cl₂): λ_{max}/nm (10⁻³ ε/mol·cm⁻¹) 301 (17), 365 (1.0), 427 (1.8), 470 (6.0), 530 (4.8), 570 (4.2). IR (cm⁻¹, KBr): 1504 ν(C=N), 918, 1006 ν(N-O).

New J. Chem., 2003, **27**, 1148–1155 **1149**

$[(n\text{-C}_4\text{H}_9)_4\text{N}]\text{Cl}$ was added. The product was extracted from the reaction mixture with chloroform (20 ml) and the chloroform extract was washed with a saturated aqueous Na_2CO_3 solution (100 ml, in 2 portions) and then with water (200 ml, in 4 portions) and dried with MgSO_4 . The chloroform solution was passed through a Silasorb SPH-300 layer (30 mm). The chloroform eluate was discarded and the desired complex was eluted with an acetonitrile–chloroform (1:3) mixture. The dark-violet solution was evaporated to dryness and the solid residue was washed with a small amount of chloroform, then with hexane and dried *in vacuo* (yield: 1.23 g, 65%). Anal. calcd. for $\text{C}_{74}\text{H}_{102}\text{N}_8\text{O}_6\text{S}_6\text{Sn}_2\text{Cl}_6\text{Fe}$: C, 46.83; H, 5.38; N, 5.91; Cl, 11.23; S, 10.14; found: C, 46.81; H, 5.43; N, 5.90; Cl, 11.14; S, 10.23%. MS(PD): m/z (positive) 2138 $[\text{M} + (n\text{-C}_4\text{H}_9)_4\text{N}]^+$. MS(MALDI-TOF): m/z (positive) 2138 $[\text{M} + (n\text{-C}_4\text{H}_9)_4\text{N}]^+$, m/z (negative) $-1413 [\text{M} - 2(n\text{-C}_4\text{H}_9)_4\text{N} + \text{H}]^-$. ^1H NMR (CD_3CN): δ 0.95 (t, 24H, CH_3), 1.34 (m, 16H, CH_2), 1.60 (m, 16H, CH_2), 3.10 (t, 16H, NCH_2), 7.20 (m, 30H, Ph). $^{13}\text{C}\{^1\text{H}\}$ NMR (CD_3CN): δ 12.8 (s, CH_3), 19.2 (s, CH_2), 23.2 (s, CH_2), 58.2 (s, NCH_2), 126.7 (s, Ph), 128.7 (s, Ph), 130.4 (s, Ph), 133.9 (s, Ph), 148.4 (s, $\text{SC}=\text{N}$). ^{119}Sn NMR [CD_3CN , rel. $\text{Sn}(\text{CH}_3)_4$]: δ -635.8 . UV-vis (CH_3CN): λ_{max} /nm ($10^{-3} \text{ } \epsilon/\text{mol}^{-1} \text{ cm}^{-1}$) 286 (26), 346 (9.2), 416 (3.1), 500 (11), 581 (7.4), 627 (7.4). IR (cm^{-1} , KBr): 1582 $\nu(\text{C}=\text{N})$, 897, 1030 $\nu(\text{N}-\text{O})$.

X-Ray crystallography

The dark-red thin-plate crystal ($0.50 \times 0.25 \times 0.06$ mm) of the $[\{(\text{CH}_3)_2\text{N}\}_4\text{P}\}_2[\text{Fe}(\text{Cl}_2\text{Gm})_3(\text{SnCl}_3)_2]$ clathrochelate, which was grown from a methylene dichloride–heptane (3:1) mixture, was a twin with a 0.62:0.38 ratio of the components as determined from the Flack parameter.¹⁵

The crystal system is orthorhombic: at 120 K $a = 19.498(9)$, $b = 8.584(4)$, $c = 29.979(13)$ Å, $U = 5018(4)$ Å³, $d_{\text{calc}} = 1.834$ g cm⁻³, $\mu = 2.026$ mm⁻¹, space group $Pna2_1$, $Z = 4$.

Intensities of 12 134 reflections ($R_{\text{int}} = 0.06$) were measured with a Bruker SMART 1K CCD area detector mounted on a 3-circle diffractometer using graphite monochromated Mo-K α radiation ($\lambda = 0.71073$ Å) by ω -scanning (step 0.35° , frame exposure time 20 s), $2\theta_{\text{max}} = 56^\circ$. The completeness of the collected reflections was 100%. Intensities of reflections were corrected using SAINT Plus and SADABS programs^{16,17} (the maximal and minimal transmission coefficients were 0.694 and 0.422, respectively).

The structure was solved by the heavy-atom method. The non-hydrogen atoms were refined by full-matrix least-squares in the anisotropic approximation except for the disordered atoms of one of the cations. The difference Fourier analysis

allowed one to elucidate and resolve positions of only the N(13), C(18), C(19), C(20) and C(22) atoms of the different cations, which were refined isotropically. For the disordered cation, the P–N and N–C bond lengths were restrained to the target values of 1.615 and 1.470 Å, respectively, with an estimated standard deviation of 0.005 Å, according to ref. 18. The positions of the hydrogen atoms were calculated geometrically with isotropic displacement parameters $U_{\text{iso}}(\text{H}) = 1.5 \cdot U_{\text{eq}}(\text{C})$, where $U_{\text{eq}}(\text{C})$ is the equivalent isotropic displacement parameter of a carbon atom. The final convergence factors were as follows: $R_1 = 0.054$ [calculated against F for 8142 reflections with $I > 2\sigma(I)$], $wR_2 = 0.127$ (calculated against F^2 for all measured reflections). All calculations were performed using the SHELXTL-97 program package.¹⁵

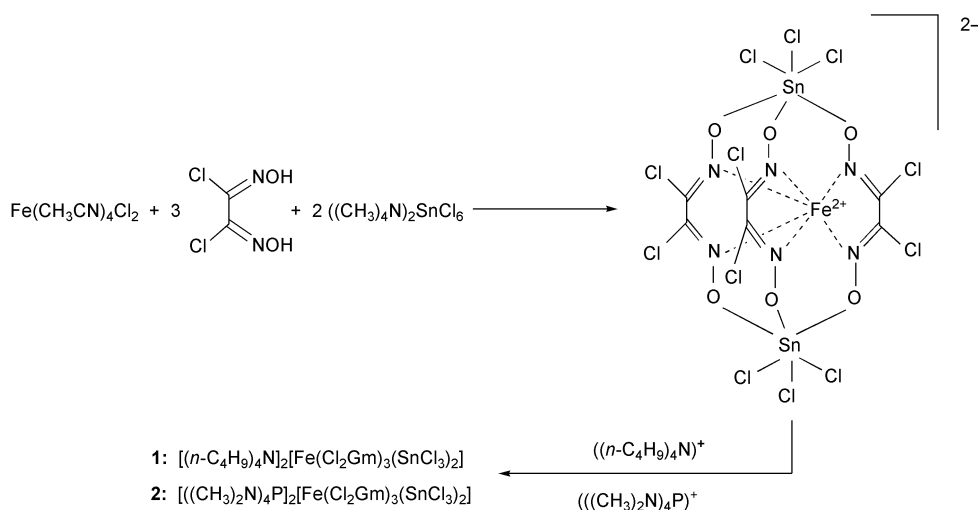
CCDC reference number 192573. See <http://www.rsc.org/suppdata/nj/b2/b211623e/> for crystallographic files in CIF or other electronic format.

Results and discussion

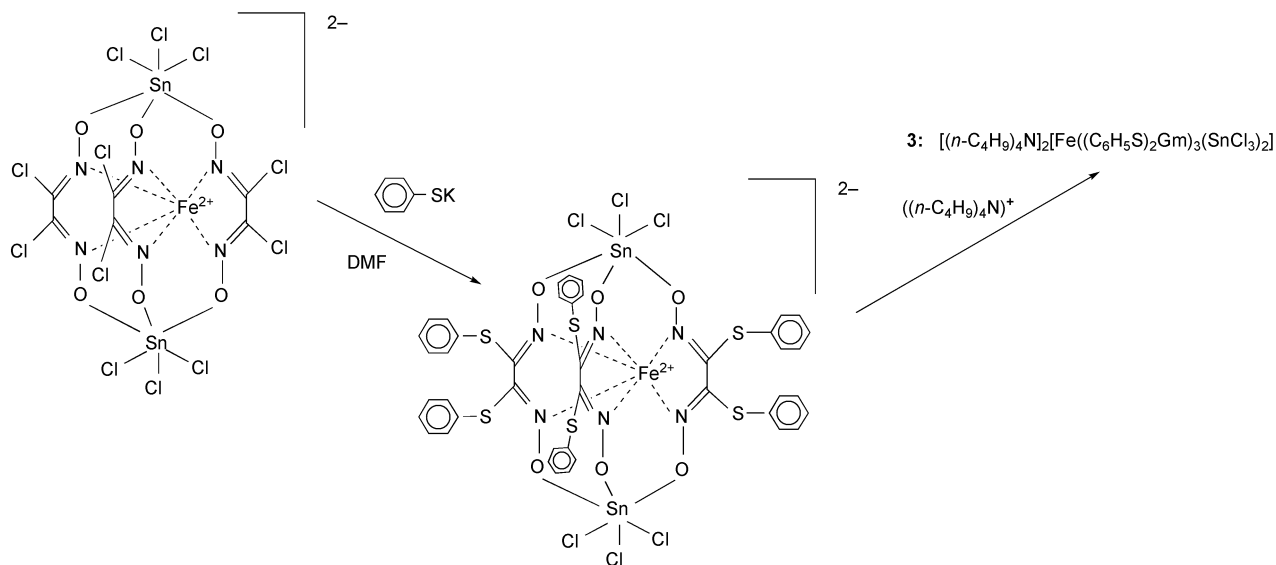
Synthesis

The tris-dichloroglyoximate clathrochelate $[\text{Fe}(\text{Cl}_2\text{Gm})_3(\text{SnCl}_3)_2]^{2-}$ dianion was synthesized by a procedure essentially different from that used earlier for its boron-capped analogs.^{1–4} Firstly, the co-ordinately saturated SnCl_6^{2-} dianion was used as the capping agent instead of boron-containing Lewis acids. Cross-linking with a similar anion, BF_4^- , was first detected for macrobicyclic phosphorus-containing tris-diiminates.¹⁹ The clathrochelate dianion formed in the course of the reaction was isolated as a tetramethylammonium salt and then, for purification, was converted to the tetra-*n*-butylammonium and tetra(dimethylamido)phosphonium salts (Scheme 2).

The tris-dichloroglyoximate tin-capped $[\text{Fe}(\text{Cl}_2\text{Gm})_3(\text{SnCl}_3)_2]^{2-}$ dianion obtained has turned out to be far less reactive than its boron-capped analogs. We have failed to unravel its interaction with sterically unhindered primary aliphatic amines (*n*-butylamine and cyclohexylamine) and alkylthiolate anions ($\text{CH}_3\text{SK}/\text{CH}_3\text{SH}$ and $n\text{-C}_4\text{H}_9\text{SH}/\text{TEA}$ systems) in DMF. The interaction of a tin-capped precursor with a phenolate anion in DMF and THF led only to the formation of a mixture of the partially substituted (mainly tri- and tetrasubstituted) products even with prolonged heating of the reaction mixture. However, with the thiophenolate anion the “regular” hexafunctionalized clathrochelate was obtained by the reaction shown in Scheme 3.



Scheme 2



Scheme 3

Structure and spectra

A crystal structure of **2** consists of one $[\text{Fe}(\text{Cl}_2\text{Gm})_3(\text{SnCl}_3)_2]^{2-}$ dianion and two $[(\text{CH}_3)_2\text{N}]_4\text{P}^+$ cations (Fig. 1), one of which is disordered.

Although quite a number of X-ray structures of boron-capped clathrochelates are known, the present paper records only the fifth tin-capped $[\text{Fe}(\text{Cl}_2\text{Gm})_3(\text{SnCl}_3)_2]^{2-}$ dianion. The structures of the other four tin-capped clathrochelates, $[(\text{C}_2\text{H}_5)_2\text{NH}_2]_2[\text{FeN}_x_3(\text{SnCl}_3)_2] \cdot [(\text{C}_2\text{H}_5)_2\text{NH}_2]^+ \cdot \text{Cl}^- \cdot 2\text{iso-C}_3\text{H}_7\text{OH}$,²⁰ $\text{H}[\text{CoDm}_3(\text{SnCl}_3)_2] \cdot 2\text{C}_6\text{H}_6$,²¹ $[(n\text{-C}_4\text{H}_9)_4\text{N}][\text{CoN}_x_3(\text{SnCl}_3)_2]$ and $[(n\text{-C}_4\text{H}_9)_4\text{N}][\text{CoDm}_3(\text{SnBr}_3)_2] \cdot \text{H}_2\text{O}$,²² where N_x^{2-} is cyclohexanedione-1,2-dioxime (nioxime) dianion and Dm^{2-} is dimethylglyoxime dianion, have been described previously. The main structural parameters for these complexes are summarized in Table 1. The N_6 -coordination polyhedra of the encapsulated metal ions in the tin-capped clathrochelates show approximate D_3 symmetry with a threefold axis passing through the capping tin atoms and encapsulated metal ion, and three twofold axes passing through this metal ion and the centres of the C–C bonds in the chelate fragments. For the complexes listed, the analogous bond lengths and bond angles are similar (Table 1). The maximal discrepancy is observed for the C–N–O angle. Its magnitude for the iron(II)

complexes (average 116.7°) is lower by approximately 3° than that for the cobalt(III) complexes (average 119.5°). Such a difference may be accounted for by a small deviation of the dioximate fragments from planar geometry as a result of distortion of the macrobicyclic ligand around its approximate C_3 axis. Twisting around this axis is characterized by a distortion angle ($\varphi = 0^\circ$ for a trigonal prism and $\varphi = 60^\circ$ for a trigonal antiprism). The distortion angle φ along with the bite angle α , the distance between the encapsulated metal ion and the coordinated nitrogen atom, and the distance h between the coordination polyhedron bases, have proven to be characteristic parameters of the geometry of macrobicyclic complexes.

Among the macrobicyclic tris-dioximates studied, clathrochelate tin-capped complexes show the maximal distortion of the macrobicyclic ligand in the direction of a TAP geometry. The distortion angle φ is largest for tin-capped cobalt(III) clathrochelates (approximately 43°) and slightly lower for the iron(II) complexes (approximately 39°) (see Table 1). The φ angle value for the tin-capped hexachloride iron(II) clathrochelate **2** is slightly higher than that for its nioximate analog. We have also observed a distortion angle φ of approximately 39° for the $[(n\text{-C}_4\text{H}_9)_4\text{N}]_2[\text{Fe}(\text{Cl}_2\text{Gm})_3(\text{SnCl}_3)_2]$ clathrochelate. Unfortunately an accurate X-ray structure of this complex has not been determined because of a complicated disordering of the cations.

The geometry of a clathrochelate complex is determined by the interaction between an encapsulated metal ion and its nearest coordination environment, in particular, the six nitrogen donor atoms.^{6,23} There are two factors, which as a matter of fact are “integral” and can be evaluated empirically. The first one is a tendency to retain a certain “optimal” distance between an encapsulated metal ion and the coordinated nitrogen atoms, and the second one is an energetic preference for a TAP coordination in comparison with a TP one for a given low-spin metal ion with a d^6 electronic configuration in terms of the ligand-field stabilization energy (LFSE) concept.

Table 1 indicates that “optimal” Fe(II)–N and Co(III)–N distances for tin-capped clathrochelates are equal to 1.92 and 1.90 Å, respectively. These values are close to the corresponding ones for the boron-capped complexes [1.91 Å for Fe(II)–N distances (more than 20 structures)⁶ and 1.89 Å for a Co(III)–N distance²⁴]. It should be noted that the realization of the ideal TP geometry by a macrobicyclic ligand in tin-capped complexes would lead to a much longer distance (approximately 2.44 Å) between metal ions and nitrogen atoms. In fact, the twisting of a coordination polyhedron

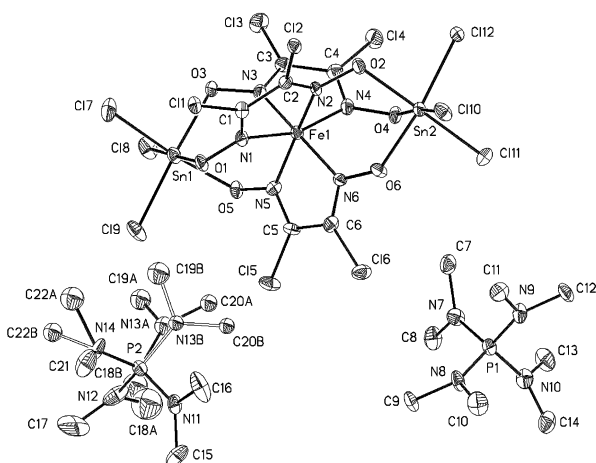


Fig. 1 View of **2** with displacement ellipsoids drawn at the 30% probability level and labelling scheme. Hydrogen atoms are not shown.

Table 1 Average structural parameters for tin-capped iron(II) and cobalt(III) tris-dioximates ($M = \text{Fe}^{\text{II}}$ or Co^{III} and $X = \text{Cl}$ or Br , depending on the compound)

	$[\text{Fe}(\text{Cl}_2\text{Gm})_3(\text{SnCl}_3)_2]^{2-}$	$[\text{FeNx}_3(\text{SnCl}_3)_2]^{2-}$	$[\text{CoNx}_3(\text{SnCl}_3)_2]^-$	$[\text{CoDm}_3(\text{SnCl}_3)_2]^-$	$[\text{CoDm}_3(\text{SnBr}_3)_2]^-$
T/K	110	183	153	298	153
$M-N/\text{\AA}$	1.915(5)	1.923	1.913	1.90	1.894
$N=C/\text{\AA}$	1.304(7)	1.300	1.283	1.29(2)	1.284
$N-O/\text{\AA}$	1.349(5)	1.376	1.346	1.37	1.337
$C-C/\text{\AA}$	1.449(7)	1.446	1.472	1.46	1.475
$C-Cl/\text{\AA}$	1.693(5)	—	—	—	—
$C-C=N/^\circ$	113.5(5)	112.5	113.2	114.1	113.1
$C=N-O/^\circ$	117.2(4)	116.2	119.5	119.4	119.5
$N-O-Sn/^\circ$	115.2(3)	115.0	114.6	114.0	115.1
$N=C-C=N^a/^\circ$	3.5	6.2	6.0	6.8	6.7
$Sn-O/\text{\AA}$	2.106(4)	2.093	2.111	2.10	2.118
$Sn-X/\text{\AA}$	2.375(2)	2.399	2.380	2.386	2.538
$M-Sn/\text{\AA}$	3.626	3.612	3.615	3.582	3.596
$h^b/\text{\AA}$	2.244(7)	2.227	2.236	2.117	2.182
$\alpha^c/^\circ$	40.5(1)	39.5	40.6	40.2	41.0
$\varphi^d/^\circ$	40.4	37.5	41.0	42.8	45.1
Reference	This work	Ref. 20	Ref. 22	Ref. 21	Ref. 22

^a Dihedral angles for the chelating fragments. ^b Distance between the coordination polyhedron bases (the height of the distorted trigonal prism).

^c Bite angle (half the chelate angle). ^d Distortion angle.

around the C_3 axis results in Fe–N and Co–N distances decreasing to “optimal” values. A slightly shorter Co(III)–N distance in comparison with the Fe(II)–N bond length is attributed to the smaller ionic (Shannon) radius of the Co^{3+} ion ($r_i = 0.68 \text{ \AA}$) in comparison to that of the Fe^{2+} ion ($r_i = 0.75 \text{ \AA}$).²⁵

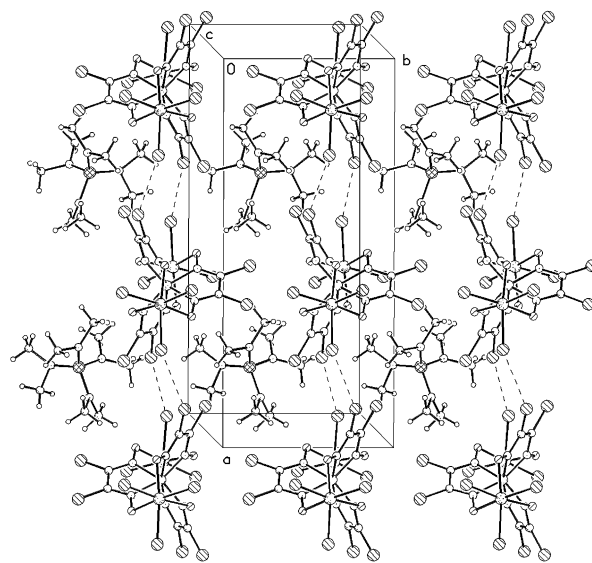
The energetic preference for a TAP geometry rather than a TP one for low-spin complexes with a metal d^6 electronic configuration was analyzed in ref. 23. This can also be considered as a factor that influences the distortion of the macrobicyclic ligand. It is in good agreement with experimental data, namely with realization of a pseudooctahedral (trigonal-antiprismatic) arrangement of the central iron(II) and cobalt(III) ions in the nonmacrocyclic $[\text{Fe}(\text{H}_2\text{Nx})_3]^{2+}$ and $[\text{Co}(\text{H}_2\text{Om})_3]^{3+}$ (where H_2Om is oxamideoxime) tris-complexes.^{26,27} It should also be noted that the metal-nitrogen distances in these complexes [1.934–1.986 \AA for Fe(II)–N bonds and 1.904–1.922 \AA for Co(III)–N bonds] are close to the upper limit for the known distances in α -dioximate complexes and are appreciably smaller than the value of 2.44 \AA expected for the ideal TP geometry in tin-capped clathrochelates.

The coordination polyhedra of the capping tin atoms in the dianion **2**, as well as in its niioximate $[\text{FeNx}_3(\text{SnCl}_3)_2]^{2-}$ analog,²⁰ also display a distorted octahedral geometry. Apart from the obvious difference in the Sn–O and Sn–Cl bond lengths, the deviation from octahedral geometry manifests itself in the increase of the Cl–Sn–Cl angles (ave. 94.7°) and decrease in the O–Sn–O angles (ave. 82.3°).

The clathrochelate dianions in the crystal of **2** form layers parallel to the crystallographic (0 0 1) plane (Fig. 2). Inside the (0 0 1) layer, a system of intermolecular $\text{Cl}\cdots\text{Cl}$ contacts between the dichloroglyoximate fragments $[\text{Cl}(1)\cdots\text{Cl}(5)^{x, 1+y}, z = 3.589(2) \text{ \AA}$ and $\text{Cl}(2)\cdots\text{Cl}(4)^{x, 1+y}, z = 3.751(2) \text{ \AA}]$ and also between the dichloroglyoximate fragments and the capping groups $[\text{Cl}(3)\cdots\text{Cl}(9)^{0.5+x, 1.5-y}, z = 3.300(3) \text{ \AA}$ and $\text{Cl}(6)\cdots\text{Cl}(12)^{-0.5+x, 1.5-y}, z = 3.441(2) \text{ \AA}]$ is observed. The tetra(dimethylamido)phosphonium cations form layers between the layers of dianions, that is, the clathrochelate **2** crystal packing can be described as an alternation of anionic and cationic layers.

Since our attempts to obtain crystals of a functionalized clathrochelate **3** suitable for an X-ray diffraction study failed, information about its electronic structure and spin state as well as the geometry of the nearest coordination environment of the encapsulated iron ion were deduced from the EXAFS spectra

and the ^{57}Fe Mössbauer parameters (for complex **1** the isomer shift, characterizing the s -electron density on the iron atom nucleus, is $\text{IS} = 0.40 \text{ mm s}^{-1}$ and the quadrupole splitting, which is determined by the electric field gradient on the iron atom nucleus, is $\text{QS} = 0.24 \text{ mm s}^{-1}$; for complex **2**: $\text{IS} = 0.40 \text{ mm s}^{-1}$ and $\text{QS} = 0.20 \text{ mm s}^{-1}$; for complex **3**: $\text{IS} = 0.35 \text{ mm s}^{-1}$ and $\text{QS} = 0.50 \text{ mm s}^{-1}$). The IS values for the compounds obtained indicate that these clathrochelates are low-spin iron(II) complexes. According to the X-ray data (see above), tin-capped clathrochelates of this type possess a geometry approaching that of a TAP, and a negative QS value has been predicted for them.^{7–10} A negative QS value was also expected for the complexes obtained. The literature QS *vs.* φ correlation relationship²⁸ and a modern version of the partial QS concept^{29,30} indicate that an increase in the distortion angle φ value leads to a decrease in the QS value. For complexes with a TP geometry and a positive QS value, this results in a decrease in the absolute QS value. TAP complexes [in particular iron(II) tris-phenanthrolinates and tris-bipyridinates] have a negative QS value (as seen from direct Mössbauer experiments in a magnetic field³¹), which increases as temperature

**Fig. 2** Packing diagram for the molecules of **2**.

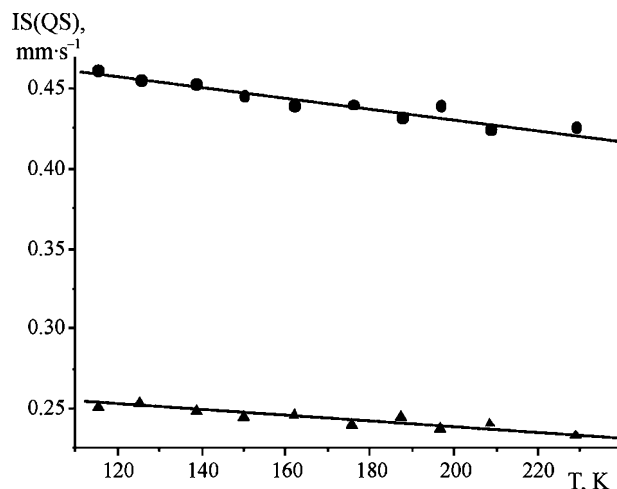


Fig. 3 The temperature dependence of the ^{57}Fe Mössbauer parameters (IS, ● and QS, ▲) for complex 1.

decreases. Since a direct determination of the sign of QS entails a considerable investigation, the sign was deduced from the temperature dependence of the ^{57}Fe Mössbauer parameters for the structurally characterized tin-capped hexachloride precursors **1** and **2** (Figs 3 and 4). As for the $[(\text{C}_2\text{H}_5)_2\text{NH}_2]_2[\text{FeN}_3(\text{SnCl}_3)_2]$ clathrochelate and the nonmacrocyclic $[\text{Fe}(\text{H}_2\text{N}_x)_3](\text{SO}_4)$ tris-nioximate,²⁰ the absolute QS values for these precursors increase with decreasing temperature, which implies a negative QS value. For the functionalized clathrochelate **3**, this corresponds to a distortion angle φ of approximately 40–50°. Thus, the geometries of the hexachloride precursors **1** and **2**, as well as that of the ribbed-functionalized clathrochelate **3**, are close to trigonal-antiprismatic.

This conclusion is also supported by the UV-vis spectra of complexes **1–3**. The geometry of the FeN_6 chromophore centre exerts an appreciable influence on the number and intensity of the $\text{M}(\text{d}) \rightarrow \text{L}(\pi^*)$ charge transfer (MLCT) bands in the visible region. The spectra of trigonal prismatic C_3 -symmetric boron-capped clathrochelates have one asymmetric band of high intensity [$\epsilon \sim (2\text{--}3) \times 10^4 \text{ mol}^{-1} \text{ l cm}^{-1}$] in this region,^{2,6,28} while the UV-vis spectra of the TAP tin-, antimony-, and germanium-capped macrobicyclic tris-dioximates in the visible region contain two or three bands of similar intensity [$\epsilon \sim (3\text{--}10) \times 10^3 \text{ mol}^{-1} \text{ l cm}^{-1}$].^{7,8,32–34} It is apparent that the UV-vis spectra of complexes **1–3** (see Experimental) are of the TAP type. The MLCT bands for the hexasulfur-containing

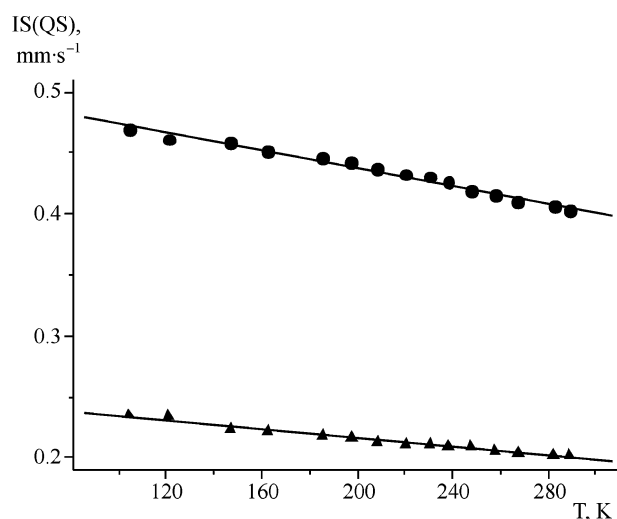


Fig. 4 The temperature dependence of the ^{57}Fe Mössbauer parameters (IS, ● and QS, ▲) for complex 2.

complex **3** are red-shifted by 30 to 50 nm compared with the hexachloride precursors **1** and **2**, as is the case for the boron-capped ribbed-functionalized clathrochelates.^{1,2}

If the ^{57}Fe Mössbauer parameters allow one to deduce the angular characteristics of the coordination polyhedron of the encapsulated iron(II) ion, the EXAFS spectra make it possible to obtain some information about distances in the clathrochelate framework. The functions for the radial distribution of atoms (RDA, see Electronic supplementary information, ESI) surrounding the scattering atom were obtained for the central iron(II) ion and also for the capping tin(IV) atom, which appreciably increases the reliability of the final results. The RDA functions were also obtained for a series of boron-capped clathrochelate analogs, the structures of which were determined previously by X-ray crystallography.^{1,2} As seen from Table 2, good agreement between the X-ray and EXAFS data is observed in most cases. For the hexasulfide complex **3**, whose X-ray structure could not be determined, by EXAFS we have determined the main distances in the clathrochelate framework to be $\text{Fe-N} \approx 1.9$, $\text{Fe-C (chelate)} \approx 2.8$, $\text{Fe-O} \approx 2.9$ and $\text{Fe-Sn} \approx 3.7 \text{ \AA}$, while in the capping tin atoms moiety $\text{Sn-O} \approx 2.1$ and $\text{Sn-Cl} \approx 2.4 \text{ \AA}$. These values are close to those found by X-ray analysis for the clathrochelate precursor **2** and the alicyclic $[\text{FeN}_3(\text{SnCl}_3)_2]^{2-}$ dianion (Table 2).

The distances from the encapsulated iron(II) ion to the sulfur atoms of the functional substituents (4.0–4.5 Å) are practically the same as those determined for the clathrochelate **3** (EXAFS experiment) and its hexasulfide boron-capped analogs (both X-ray and EXAFS experiments).

The ^1H and $^{13}\text{C}\{^1\text{H}\}$ NMR as well as PD and MALDI-TOF mass spectra of the synthesized complexes confirm their composition and C_3 symmetry; the parameters of the ^{119}Sn NMR spectra of these clathrochelates indicate a high symmetry of the octahedral SnCl_3O_3 capping fragment.

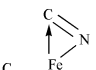
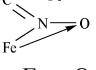
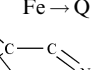
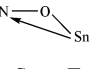
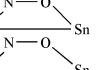
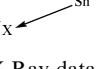
Electrochemistry

Cyclic voltammograms of the iron(II) clathrochelates are characterized by the existence of an anodic wave, which is assigned to the oxidation of the encapsulated iron(II) to iron(III).⁶ The half-wave potential value, $E_{1/2}$, for the $\text{Fe}^{3+/2+}$ couple depends on the electron-donating properties of the substituents at the capping atoms and in the ribbed fragments. The reversibility of the electrochemical reactions might be characterized by the Tomeš criterion value, ΔE , which is determined as $\Delta E = E_{3/4} - E_{1/4}$ and is equal to 56 mV for a one-electron reversible process. As seen from Table 3, the tin-capped clathrochelates are oxidized at lower potentials than their boron-capped analogs. Furthermore, the Tomeš criterion value and the cyclability indicate a higher reversibility of the redox processes for the former complexes. This might be due to an increase in electron density on the encapsulated iron ion, resulting from the 2– formal charge of the capping SnCl_3O_3 groups, which delocalized onto the clathrochelate framework through the σ and π bond systems.

Conclusion

The hexachloride TAP tin-capped precursor obtained is less reactive than its boron-capped analogs. This is ascribed to an increase in the electron density of the capping group. The BRO_3 fragment has a formal charge equal to 1–, while the capping SnCl_3O_3 group has a formal charge of 2–. Such electron density changes influence the clathrochelate framework through the system of σ and π -conjugated bonds and the electron density on the carbon azomethine atoms of the chelate fragments also increases. As a result, the reactivity of the dichloroglyoximate fragments in nucleophilic substitution reactions decreases and only a limited number of functionalized

Table 2 X-Ray^a and EXAFS data on distances (Å) from the encapsulated iron(II) ion and capping Q atoms for boron- and tin-capped clathrochelate iron(II) dioximates (cn is coordination number)

	cn	Fe(Cl ₂ Gm) ₃ (Bn-C ₄ H ₉) ₂ ²⁻	Fe(Cl ₂ Gm) ₃ (BC ₆ H ₅) ₂ ¹	Fe{(CH ₃ S) ₂ Gm} ₃ (BC ₆ H ₅) ₂ ²⁻	Fe{(C ₆ H ₅ S) ₂ Gm} ₃ (BC ₆ H ₅) ₂ ¹	[Fe(Cl ₂ Gm) ₃ (SnCl ₃) ₂] ²⁻	[Fe{(C ₆ H ₅ S) ₂ Gm} ₃ (SnCl ₃) ₂] ²⁻	[FeN _x ₃ (SnCl ₃) ₂] ²⁻ ^{9,20}
Fe → N	6	1.92 (1.90)	1.92 (1.91)	1.92 (1.90)	1.92 (1.91)	1.91 (1.90)	1.92	1.93 (1.92)
	6	2.75 (2.75)	2.84 (2.74)	2.87 (2.78)	2.85 (2.77)	2.78 (2.74)	2.78	2.80 (2.78)
	6	2.90 (2.90)	3.01 (2.91)	3.00 (2.89)	2.95 (2.88)	2.94 (2.92)	2.94	3.05 (2.94)
Fe → Q	2	3.01 (3.04)	3.04 (3.08)	3.04 (3.00)	3.06 (3.01)	3.68 (3.63)	3.67	3.60 (3.61)
	6	4.30 (4.39)	4.29 (4.39)	4.36 (4.47)	4.35 (4.46)	4.23 (4.39)	4.33	4.32 (4.24)
Sn → O	3					2.12 (2.11)	2.13	(2.10)
Sn → Ck	3					2.38 (2.37)	2.41	(2.40)
	3					3.38 (2.95)	3.41	(2.96)
Sn → Fe	2					3.64 (3.63)	3.62	(3.61)
	3					3.91 (3.99)	4.19	(4.00)
	3					4.43 (4.64)	4.33	(4.54)

^a X-Ray data are given in parentheses when available.**Table 3** Electrochemical characteristics for boron- and tin-capped iron(II) clathrochelates

Compound	<i>E</i> _{1/2} /mV	Tomeš criterion/mV
Fe(Cl ₂ Gm) ₃ (BF) ₂ ²⁻	1415	65
Fe(Cl ₂ Gm) ₃ (BC ₆ H ₅) ₂ ²⁻	1360	80
Fe(Cl ₂ Gm) ₃ (Bn-C ₄ H ₉) ₂ ²⁻	1320	90
Fe{(C ₆ H ₅ S) ₂ Gm} ₃ (BC ₆ H ₅) ₂ ²⁻	895	80
[Fe(Cl ₂ Gm) ₃ (SnCl ₃) ₂] ²⁻	890	60
[Fe{(C ₆ H ₅ S) ₂ Gm} ₃ (SnCl ₃) ₂] ²⁻	500	60

complexes can be synthesized. In this connection, we believe that in order to obtain a wider range of TAP clathrochelates, it will be necessary to synthesize TAP triorganylantimony-capped halogenide precursors in which the capping SbR₃O₃ fragment has a formal charge of 1–,³² from which a higher reactivity of these precursors in the nucleophilic substitution reactions can be expected.

Acknowledgements

Support of the Russian Foundation for Basic Research (Grants N99-03-32498, 00-03-32807, 00-03-32578 and 03-32531) is gratefully acknowledged.

References

- Y. Z. Voloshin, O. A. Varzatskii, A. V. Palchik, A. I. Stash and V. K. Belsky, *New J. Chem.*, 1999, **23**, 355.
- Y. Z. Voloshin, O. A. Varzatskii, T. E. Kron, V. K. Belsky, V. E. Zavodnik and A. V. Palchik, *Inorg. Chem.*, 2000, **39**, 1907.
- Y. Z. Voloshin, V. E. Zavodnik, O. A. Varzatskii, V. K. Belsky, A. V. Palchik, N. G. Strizhakova, I. I. Vorontsov and M. Y. Antipin, *J. Chem. Soc., Dalton Trans.*, 2002, 1193.
- Y. Z. Voloshin, O. A. Varzatskii, T. E. Kron, V. K. Belsky, V. E. Zavodnik, N. G. Strizhakova, V. A. Nadtochenko and V. A. Smirnov, *J. Chem. Soc., Dalton Trans.*, 2002, 1203.
- Y. Z. Voloshin, O. A. Varzatskii, T. E. Kron and A. V. Palchik, *XXVII International Symposium on Macrocyclic Chemistry*, Park City, UT, USA, June 23–27, 2002.
- Y. Z. Voloshin, N. A. Kostromina and R. Krämer, *Clathrochelates: Synthesis, Structure and Properties*, Elsevier, Amsterdam, 2002.
- Y. Z. Voloshin, N. A. Kostromina, A. Y. Nazarenko and E. V. Polshin, *Inorg. Chim. Acta*, 1991, **185**, 83.
- Y. Z. Voloshin, V. V. Trachevskii and E. V. Polshin, *Pol. J. Chem.*, 1997, **71**, 428.
- Y. Z. Voloshin, O. A. Varzatskii, E. Y. Tkachenko, Y. A. Maletin, S. P. Degtyarov and D. I. Kochubey, *Inorg. Chim. Acta*, 1997, **255**, 255.
- Y. Z. Voloshin, A. I. Stash, O. A. Varzatskii, V. K. Belsky, Y. A. Maletin and N. G. Strizhakova, *Inorg. Chim. Acta*, 1999, **284**, 180.
- G. Ponzio and F. Baldracco, *Gazz. Chim. Ital.*, 1930, **60**, 415.
- A. J. Bard and L. R. Faulkner, *Electrochemical methods: fundamentals and applications*, Wiley, New York, 2nd edn., 2001.
- K. V. Klementev, *Nucl. Instrum. Methods Phys. Res. A*, 2000, **448**, 299.
- S. J. Gurman, N. Binsted and I. Ros, *J. Phys. C*, 1986, **19**, 1845.
- G. M. Sheldrick, *SHELXTL-97. Program for Solution and Refinement of Crystal Structure*, Bruker AXS Inc., Madison, WI, USA, 1997.
- SMART and SAINT, Release 5.0, Area Detector Control and Integration software*, Bruker AXS Inc., Madison, WI, USA, 1998.
- G. M. Sheldrick, *SADABS: A Program for Exploiting the Redundancy of Area-Detector X-ray Data*, University of Göttingen, Göttingen, Germany, 1999.
- F. H. Allen, O. Kennard, D. G. Watson, L. Brammer, A. G. Orpen and R. Taylor, *J. Chem. Soc., Perkin Trans. 2*, 1987, S1.
- J. E. Parks, B. E. Wagner and R. H. Holm, *Inorg. Chem.*, 1971, **10**, 2472.
- S. V. Lindeman, Y. T. Struchkov and Y. Z. Voloshin, *J. Coord. Chem.*, 1993, **28**, 319.
- Y. Z. Voloshin, V. K. Belsky and V. V. Trachevskii, *Polyhedron*, 1992, **11**, 1939.
- S. V. Lindeman, V. T. Struchkov and Y. Z. Voloshin, *J. Coord. Chem.*, 1995, **34**, 203.
- E. Larsen, G. N. La Mar, E. B. Wagner and R. H. Holm, *Inorg. Chem.*, 1972, **11**, 2652.
- G. A. Zakrzewski, C. A. Chilardi and E. C. Lingafelter, *J. Am. Chem. Soc.*, 1971, **93**, 4411.
- B. K. Vainshtein, V. M. Fridkin, V. L. Idenbom, *Comprehensive Crystallography*, Nauka, Moscow, 1979, vol. 2.

- 26 Y. A. Simonov, A. A. Dvorkin, T. I. Malinovskii, V. K. Belsky, I. I. Bulgak, D. G. Batir and L. D. Ozol, *Koord. Khim.*, 1985, **11**, 1554.
- 27 O. Bekaroglu, S. Sarisaban, A. R. Koray, B. Nuber, K. Weidenhammer, J. Weiss and M. L. Ziegler, *Acta Crystallogr., Sect. B*, 1978, **34**, 3591.
- 28 Y. Z. Voloshin, N. A. Kostromina and A. Y. Nazarenko, *Inorg. Chim. Acta*, 1990, **170**, 181.
- 29 A. Y. Nazarenko, E. V. Polshin and Y. Z. Voloshin, *Mendeleev Commun.*, 1993, 45.
- 30 Y. Z. Voloshin, E. V. Polshin and A. Y. Nazarenko, *Hyperfine Interact.*, 2002, **141–142**, 309.
- 31 W. M. Reiff, *J. Am. Chem. Soc.*, 1973, **95**, 3048.
- 32 Y. Z. Voloshin, O. A. Varzatskii, S. V. Korobko and Y. A. Maletin, *Inorg. Chem. Commun.*, 1998, **1**, 328.
- 33 Y. Z. Voloshin and E. V. Polshin, *Polyhedron*, 1992, **11**, 457.
- 34 Y. Z. Voloshin, O. A. Varzatskii, N. G. Strizhakova and E. Y. Tkachenko, *Inorg. Chim. Acta*, 2000, **299**, 104.